VNU Journal of Science: Mathematics - Physics

Journal homepage: https://js.vnu.edu.vn/MaP

Original Article

One-step Spray Coating $CsPbBr_3$ Film for Planar Photodetector Applications

Bui Xuan Thanh[1], Tran Phuong Nam[1], Tran Quoc Hoan[1,2], Pham Van Tuan[1], Duong Thanh Tung[1,*]

[1]*Hanoi University of Science and Technology (HUST), 1 Dai Co Viet, Hanoi, Vietnam*

[2]*Electric Power University, 235 Hoang Quoc Viet, Hanoi, Vietnam*

Received 01 January 2023
Revised 23 February 2023; Accepted 24 February 2023

Abstract: Metal halide perovskite, a promising semiconducting material, is suitable for new-generation optoelectronic applications. Compared to organic-inorganic hybrid perovskites (OIHP), all inorganic $CsPbX_3$ (X = Cl, Br, and I) show superior thermal and chemical stability. However, the fabrication process of $CsPbX_3$ is conventionally involved with spin coating, while the $CsPbBr_3$ precursor dissolubility is very low compared to OIHP. Consequently, low materials utilization and poor uniformity for the large-scale area can be obtained, which limits the application of $CsPbBr_3$ in producing quantum dots (QDs) perovskite film. In this work, we report a facile spray coating method to produce $CsPbBr_3$ film on a pre-patterned Pt electrode for photodetector (PD) application. The spray-coated perovskite was suitable for photodiode outstanding properties such as a high responsivity of 60 A/W, high detectivity of 6×10^{-13} J., the response time (rising and fall time) below 17 ms were obtained at 1 V under 405 nm illumination. Results of this work show that the spray deposition technique will benefit further thin film-based perovskite optoelectronic devices.

Keywords: Spray coating method, photodetectors, $CsPbBr_3$ film.

1. Introduction

Over the past several years, organic-inorganic hybrid perovskites (OIHPs) have emerged as an active material for thin-film optoelectronic applications such as solar cells, light emitting diode, photodetector, etc. [1-3]. These semiconductors have unique electro-photoluminescence properties, such as long carrier

* Corresponding author.
E-mail address: tung.duongthanh@hust.edu.vn

https//doi.org/10.25073/2588-1124/vnumap.4795

diffusion length, high absorption coefficients, and low defect states. In photovoltaics, the power conversion efficiency of perovskite solar cells has been demonstrated to possibly reach over 24%, which is the largest among next-generation solar cells [4-8]. They also have the potential, in combination with traditional silicon batteries, to achieve an overall efficiency of over 28% [9-10]. Perovskite thin films have also been adopted as the luminescent layer in light-emitting diodes (LEDs). By controlling the film crystallization process and/or mixing halogen anionic in perovskite nanocrystals, the external quantum efficiency (EQE) can be improved to over 20%. However, the OIHPs suffer from problems related to poor water and thermal stability that limit their practical applications [11]. Compared to organic-inorganic hybrid perovskites, all inorganic $CsPbX_3$ (X = Cl, Br, and I) show superior thermal and chemical stability [12-16]. Currently, most $CsPbX_3$ perovskite thin film fabrication studies focus on solution processing techniques; because they are simple, easy to implement at low temperatures, and large scale processability. One scalable deposition strategy of solution processing for depositing high-quality perovskite thin films is spray coating which has been proven to be an effective technique for fabricating optoelectronic devices with multilayer stacks. Traditional commercial photodetector based on silicon single-crystal p-i-n junction with ultrafast response time (nanosecond scale) and ultralow dark current density (picoampere scale); however, due to its low absorbance coefficient and indirect bandgap, the light responsivity is limited at < 0.55A/W at the peak wavelength of 940 nm (near-infrared range) [17]. Thus, responsivity and detectivity levels of perovskite photodetectors have exceeded those of conventional photodetector technologies (e.g. silicon-based) under an applied bias (especially in UV-Visible light) [18]. In a previous work [17], we successfully fabricated the perovskite $CH_3NH_3PbI_3$ film employing a facile CNC-assisted spray coating method for solar cell application. Spray deposition at the optimal spray rate and substrate temperature produces a large-grain-size and void-free methylammonium lead iodide ($MAPbI_3$) bilayer structure. When the films are incorporated into a solar cell device with a conductive carbon counter electrode, a maximum power conversion efficiency of 10.58% was obtained [19-21].

In this work, we report a systematic approach to prepare uniform and crystalline $CsPbBr_3$ perovskite thin films with complete surface coverage via one step hot spray coating process of CsBr and $PbBr_2$ precursors. The ratio between the two precursors was found to play a critical role in enhancing the photoluminescence efficiency of the deposited perovskite thin films. The resulting perovskite photodiode achieved a figure of merits for photodetector application.

2. Experimental

2.1. Samples Preparation

Materials: All reagents were used without further purification. Lead bromide ($PbBr_2$, 99.9% metal basis), cesium Bromide (CsBr, 99.9% metal basis), NN Dimethyl formamide (DMF, > 99%, analytical grade) were bought from Macklin Chemical.

First, 0.25 mmol of CsBr and $PbBr_2$ were mixed in DMF solvent at various mol ratios of 1/1.2; 1/1; 1.2/1 with magnetic stirring until completely dissolved.

Spray coating $CsPbBr_3$ NCs film on Pt electrodes: The planar integrated Ti/Pt (50/200 nm) electrode is fabricated using standard photolithography to pattern the photoresist for subsequent metallization and lift-off. The electrode includes 40 fingers with the channel width and lengths of 20 μm and 1.60 mm, respectively. The total active area was 0.128 mm^2.

Prior to coating, pre-patterned Pt electrodes on SiO_2/Si substrate were ultrasonically cleaned in acetone and ethanol for 10 min and dried in the oven at 100 °C for 30 min. The precursors were

introduced onto the pre-patterned Pt electrodes on SiO_2/Si substrate via the air-brushed sprayer (spray type: 74510, Japan) at a substrate temperature of 220 °C in order to achieve uniformity perovskite films. The N_2 gas pressure was fixed at ~ 103.43 Pa, and the spraying volume was controlled at 5 µL/min. Films were sprayed at nozzle heights fixed at 60 mm with a lateral moving speed between 1.0 cm/s, the scanning steps at 2 mm, and the spray angle between the nozzle with the basal is 75-80°.

2.2. Analytical Methods

The surface and cross-section morphologies of perovskite layers were analyzed using scanning electron microscopy (SEM, JEOL). The current–voltage (I-V) characteristics of the devices were obtained by applying a potential external bias to the devices and measuring the generated photocurrent with a Keithley model 4200 digital source meter (Keithley, USA) under illumination from a 405 nm laser coupled with a pulse generator. A 450 W monochromatic light source Xe arc and spectrometer (NanoLog, Horiba) measured excitation and fluorescence emission results at room temperature.

3. Results and Discussion

3.1 Physical Properties of Spray-coated $CsPbBr_3$ Film

The surface and cross-section morphologies of as-prepared $CsPbBr_3$ film coated on 600 nm Fluoride doped Tin Oxide (FTO) substrate with $CsBr/PbBr_2$ mol ratio of 1/1 were obtained via scanning electron microscopy (SEM) as shown in Fig. 1. Both surface and cross-section images showed dense packaging and compact, crack-free $CsPbBr_3$ films. Additionally, the particles with an average size of 200 nm and an approximately 250 nm-thick film can be observed to adhere directly to the FTO substrate.

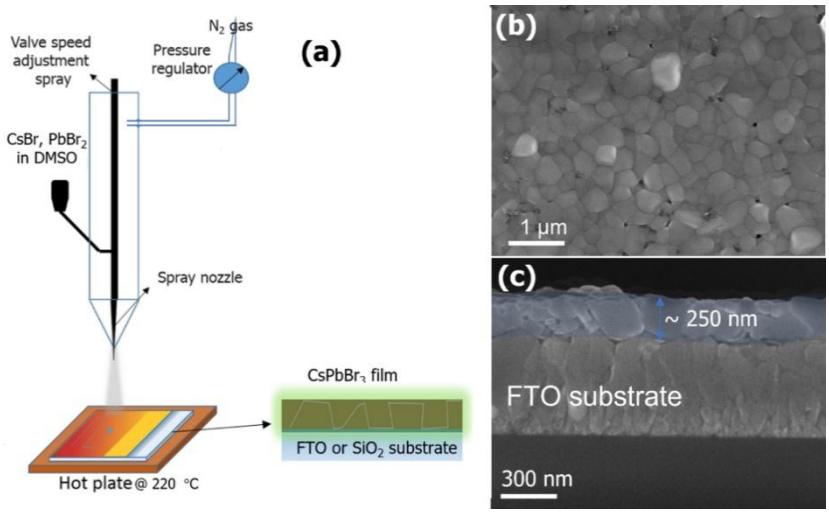

Figure 1. Diagram of (a) spray-coated $CsPbBr_3$ film procedure and (b-c) SEM images of spray-coated $CsPbBr_3$ films with $CsBr/PbBr_2$ mol ratio of 1/1 on FTO substrate.

Three perovskite samples with different molar ratios of CsBr and $PbBr_2$ (1.2:0.8, 1:1, 0.8:1.2) were produced to investigate the characteristics of thin films further. X-ray diffraction (XRD) measurements were used to analyze the crystal structures of the prepared spray-deposited perovskite films, as shown in Fig. 2. All three samples exhibited a pure cubic phase (PDF# 54-0752) with diffraction peaks at 15.2°,

21.6°, 30.6°, 34.4°, and 38.0°, corresponding to the (101), (121), (202), (141), and (321) crystal planes, which can confirm the integrity of the perovskite structure. The lattice parameter is consistent with several previous reports. The characteristic peaks of CsBr and $PbBr_2$ could not be observed, suggesting that the change in film stoichiometry has an insignificant effect on the crystal structure of the deposited films. The morphology of the $CsPbBr_3$ perovskite films is investigated by conducting top-section and cross-section SEM, as shown in Fig. 1.

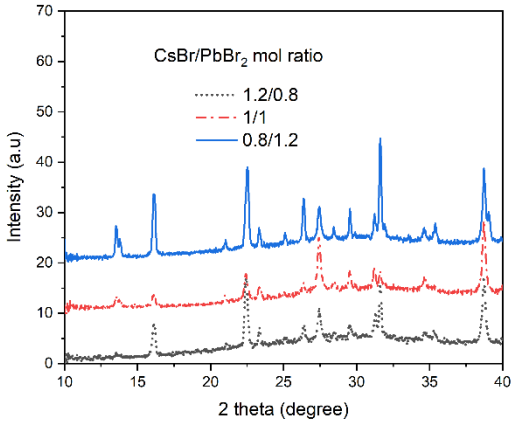

Figure 2. XRD patterns of spray-coated $CsPbBr_3$ films with different $CsBr/PbBr_2$ mol ratios.

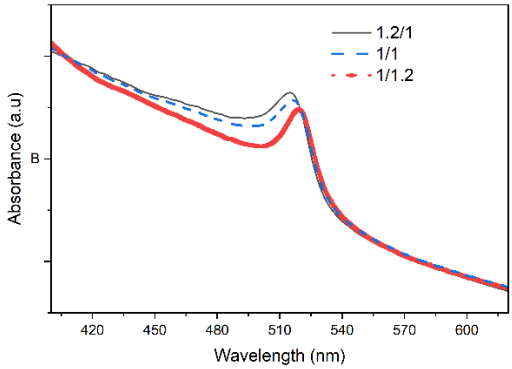

Figure 3. The absorbance spectra of spray-coated $CsPbBr_3$ films with different $CsBr/PbBr_2$ mol ratios.

The optical absorption of the as-prepared spray-coated $CsPbBr_3$ samples was prepared to understand further the influence of $CsBr/PbBr_2$ on the optical properties of $CsPbBr_3$. The absorbance peak of samples slightly shifted from 515 nm to 519 and 521 nm, corresponding to 1.2/1, 1:1, and 1:1.2 $CsBr/PbBr_2$ mol feed ratio of precursors, respectively (Fig. 3).

3.2 Photodetector Characteristics of Spray-Coated $CsPbBr_3$ Film

A 405 nm laser diode was employed as the light source to illuminate the photodetectors on the sample stage with a spot size of ~ 0.75 mm in radius to determine the photoresponse. The corresponding power intensity of light sources was measured at 0.1 mW/cm^2. Under light illumination, photocurrent can be generated via a photoconductive effect, and a Keithley 4200 system can subsequently record the relationship between photocurrent and voltage. Regarding the response time measurement, the curve of

photocurrent versus time was recorded as periodically turned on/off laser diodes, the pulse generator (1 Hz-1 MHz are used to power the laser light source). The response time can be evaluated by measuring the duration between 10% and 90% of the maximum photocurrent.

Moreover, the area of the photodetector is essential, as it directly affects the device's performance. The active area can be defined as the area between two electrodes for the photodetectors with a lateral structure. In this work, the active area was to be calculated at 128 μm^2. The structure diagram of the measuring system is described as shown in Fig. 4.

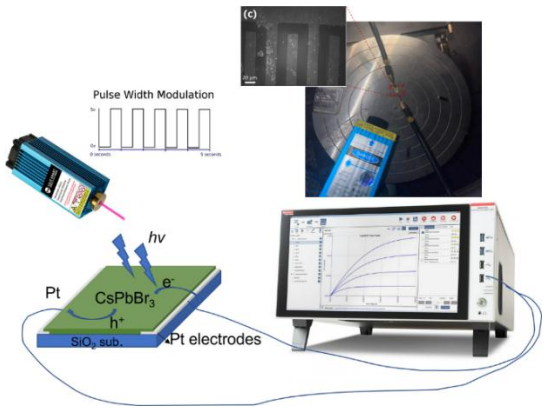

Figure 4. Schematic diagram of Photodetector measurement.

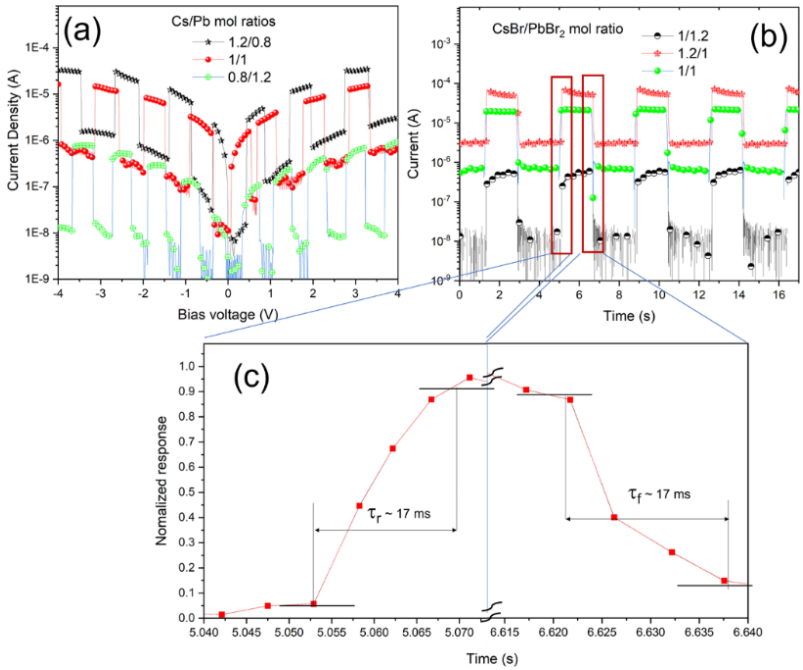

Figure 5. (a) Logarithmic I–V curves of photodetectors in the dark and under irradiation, (b) and (c) The response and recovery time analysis of the photodetectors at 1 V (405 nm@ 0.1 mW/cm^2).

Fig. 5a shows the current–voltage profile curves of samples fabricated by spraying with different $CsBr/PbBr_2$ ratios. As shown in Fig. 5a, the on-off current ratios of the samples remain almost

unchanged with the bias sweep external voltage potential from - 4 to + 4 V. Fig. 5b shows the time-sensitive line of samples at an external voltage of 1 V. Samples with CsBr/$PbBr_2$ ~1/1.2 and 1/1 ratios had ~ 40 times, while CsBr/$PbBr_2$ ~1.2/1 samples had only ~ 10 times. This is maybe because of the excess of Cs^- ions, causing the formation of a small amount of insulating Cs_4PbBr_6 phase (could not be observed by XRD patterns) [22].

Photoresponse features have been plotted to infer the rise time (τ_r: time taken for the photocurrent to rise from 10 to 90% of its amplitude) and decay time (τ_f: time taken for the photocurrent to drop from 90 to 10% of its amplitude). Devices' rise and decay times were evaluated at about ~ 17 ms for all three samples. Typically, the speed of response of devices corresponds to the scale of the carrier lifetimes of the $CsPbBr_3$ NCs film. Because of limitations of the apparatus employed to acquire the photocurrent during the transient measurements, these rise and fall times should not be regarded as the absolute response speed of our photodetectors, and hence the actual t_{on} and t_{off} are indeed shorter than 17 ms.

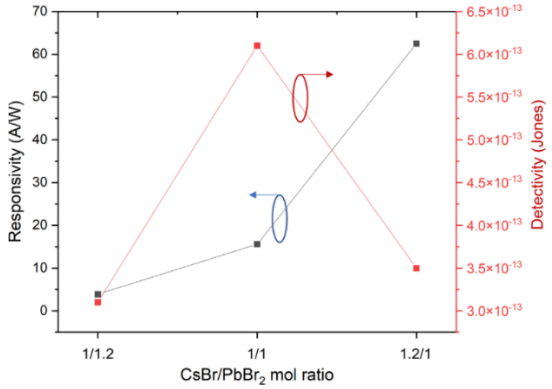

Figure 6. Dependences of Responsivity and Specific detectivity on different CsBr/$PbBr_2$ mol ratios.

Table 1. Comparison of device performance of $CsPbBr_3$ -based photodetectors

Active Materials	Wavelength (nm)	Responsivity (A/W)	Rise/fall (s)	On/off ratio	Detectivity (Jones)	ref
$CsPbBr_3$ QDs	0.40 mWcm^{-2} @ 532 nm	4.7x10^{-3}	0.2/1.3	1.6x10^5	16.84x10^8	[14]
$CsPbBr_3$ micro-particles	1.01 mWcm^{-2} @ 442 nm	0.18	1.8/1	8x10^3	6.1x10^{10}	[20]
$CsPbBr_3$ nanosheets	0.35 mWcm^{-2} @ 442 nm	0.25	0.019/0.025	10^3	-	[22]
Single crystal $CsPbBr_3$	1 mW @ 450 nm	0.028	90.7/57	10^2	1.8x10^{11}	[22]
$CsPbBr_3$ spray coating	405 nm @ 0.1 mW/cm^2	60	< 17 ms	10^2	3.6 ×10^{13}	this work

Two important parameters of the device, the responsivity (R) and Detectivity (D*), can be obtained from equation $R = I_{ph}/P_{light}$ [3] where I_{ph} is the photocurrent, P_{light} is the light power intensity (0.1 mWcm^{-2}). $D = R/\sqrt{2qI_{dark}}$, where I_{dark} is dark current, q is the elementary charge (Coulomb). The highest values achieved for responsivity and specific detectivity were 60 A/W with the CsBr/$PbBr_2$ mol ratio of 1.2/1; However, the detectivity of the sample (~3.6×10^{-3} Jones) is slightly lower than the sample with the CsBr/$PbBr_2$ mol ratio of 1/1 (6.1 × 10^{13} Jones), when the devices were exposed to 405 nm laser LED

illumination with intensity at 0.1 $mWcm^{-2}$. The analytical parameters of $CsPbBr_3$-based photodetectors are summarized in Table 1. The superior performance obtained from photodetectors via spray-deposited perovskite NCs films might be attributed to the high intrinsic quality of the perovskite films (high-quality compact films with no pinholes).

4. Conclusion

We successfully fabricated $CsPbBr_3$ films on pre-patterned $Pt/SiO_2/Si$ substrate as a planar photodetector with metal/Semiconductor/metal structure via a one-step spray coating method with different $CsBr/PbBr_2$ mol ratio of 1/1.2, 1/1, and 1/1.2. The compact, crack-free $CsPbBr_3$ films with an average particle size of 200 nm and an approximately 250 nm-thick film can be observed to adhere directly to the pre-patterned Pt electrodes on SiO_2/Si substrate. Consequently, the photodetector device performance shows several figures of merits, such as an on/off ratio of 10^2 times, responsivity of 60 $A.W^{-1}$, and Detectivity of 6.1×10^{13} Jones (by using 0.1 $mWcm^2$ 405 nm LED light source). The obtained results suggest that this technique is a potential method for fabricating high-quality all-inorganic perovskite films for photodetector application.

Acknowledgments

This research is funded by the Vietnamese National Foundation for Science and Technology Development (NAFOSTED) under grant number 103.02-2020.46.

References

[1] Y. Li, Z. F. Shi, S. Li, L. Z Lei, H. F. Ji, D. Wu, T. T. Xu, Y. T. Tian, X. J. Li, High-performance Perovskite Photodetectors Based on Solution-processed All-inorganic $CsPbBr_3$ Thin Films, Journal of Materials Chemistry C, Vol. 5, No. 33, 2017, pp. 8355-8360, https://doi.org/10.1039/C7TC02137B.

[2] Z. Yang, M. Wang, J. Li, J. Dou, H. Qiu, J. Shao, Spray-Coated $CsPbBr_3$ Quantum Dot Films for Perovskite Photodiodes, ACS Applied Materials and Interfaces, Vol. 10, No. 31, 2018, pp. 26387-26395, https://doi.org/10.1021/acsami.8b07334.

[3] H. Zhou, L. Fan, G. He, C. Yuan, Y. Wang, S. Shi, N. Sui, B. Chen, Y. Zhang, Q. Yao, J. Zhao, X. Zhang, J. Yin, Low Defects, Large Area and High Stability of All-inorganic Lead Halide Perovskite Cspbbr3 Thin Films with Micron-grains: Via Heat-spraying Process for Self-driven Photodetector, RSC Advances, Vol. 8, No. 51, 2018, pp. 29089-29095, https://doi.org/10.1039/C8RA04558E.

[4] X. Liu, Z. Liu, J. Li, X. Tan, B. Sun, H. Fang, S. Xi, T. Shi, Z. Tang, G. Liao, Ultrafast, Self-powered and Charge-transport-layer-free Photodetectors Based on High-quality Evaporated Cspbbr3 Perovskites for Applications in Optical Communication, Journal of Materials Chemistry C, Vol. 8, No. 10, 2020, pp. 3337-3350, https://doi.org/10.1039/C9TC06630F.

[5] J. Duan, D. Dou, Y. Zhao, Y. Wang, X. Yang, H. Yuan, B. He, Q.Tang, Spray-assisted Deposition of $CsPbBr_3$ Films in Ambient Air for Large-area Inorganic Perovskite Solar Cells, Materials Today Energy, Vol. 10, 2018, pp. 146-152, https://doi.org/10.1016/j.mtener.2018.09.001.

[6] L. Zhou, K. Yu, F. Yang, J. Zheng, Y. Zuo, C. Li, B. Cheng, Q. Wang, All-inorganic Perovskite Quantum Dot/Mesoporous TiO_2 Composite-based Photodetectors with Enhanced Performance, Dalton Transactions, Vol. 46, No. 6, 2017, pp. 1766-1769, https://doi.org/10.1039/C6DT04758K.

[7] S. V. N. Pammi, R. Maddaka, V. D. Tran, J. H. Eom, V. Pecunia, S. Majumder, M. D. Kim, S. G. Yoon, CVD-deposited Hybrid Lead Halide Perovskite Films for High-responsivity, Self-powered Photodetectors with Enhanced Photo Stability Under Ambient Conditions, Nano Energy, Vol. 74, 2020, pp. 104872, https://doi.org/10.1016/j.nanoen.2020.104872.

[8] X. Tang, Z. Zu, Z. Zang, Z. Hu, W. Hu, Z. Yao, W. Chen, S. Li, S. Han, M. Zhou, $CsPbBr_3$/Reduced Graphene Oxide Nanocomposites and Their Enhanced Photoelectric Detection Application, Sensors and Actuators, B: Chemical, Vol. 245, 2017, pp. 435-440, https://doi.org/10.1016/j.snb.2017.01.168.
[9] Y. Dong, Y. Gu, X. Zou, J. Song, L. Xu, J. Li, J. Xue, X. Li, H. Zeng, Improving All-Inorganic Perovskite Photodetectors by Preferred Orientation and Plasmonic Effect, Small, Vol. 12, 2016, pp. 5622-5632, https://doi.org/10.1002/smll.201602366.
[10] X. Li, D. Yu, F. Cao, Y. Gu, Y. Wei, Y. Wu, H. Zeng, Healing All-Inorganic Perovskite Films via Recyclable Dissolution-Recyrstallization for Compact and Smooth Carrier Channels of Optoelectronic Devices with High Stability, Advanced Functional Materials, Vol. 26, No. 32, 2016, pp. 5903-5912, https://doi.org/10.1002/adfm.201601571.
[11] J. Song, L. Xu, J. Li, J. Xue, Y. Dong, X. Li, H. Zeng, Monolayer and Few-Layer All-Inorganic Perovskites as a New Family of Two-Dimensional Semiconductors for Printable Optoelectronic Devices, Adv. Mater., Vol. 28, No. 24, 2016, pp. 4861-4869, https://doi.org/10.1002/adma.201600225.
[12] J. Ding, S. Du, Z. Zuo, Y. Zhao, H. Cui, X. Zhan, High Detectivity and Rapid Response in Perovskite $CsPbBr_3$ Single-Crystal Photodetector, J. Phys. Chem. C, Vol. 121, No. 9, 2017, pp. 4917-4923, https://doi.org/10.1021/ACS.JPCC.7B01171.
[13] O. Y. Gong, M. K. Seo, J. H. Choi, S. Y. Kim, D. H. Kim, I. S. Cho, N. G. Park, G. S. Han, H. S. Jung, High-performing Laminated Perovskite Solar Cells by Surface Engineering of Perovskite Films, Applied Surface Science, Vol. 591, 2022, pp. 153148, https://doi.org/10.1016/j.apsusc.2022.153148.
[14] D. Liu, Y. Guo, M. Que, X. Yin, J. Liu, H. Xie, C. Zhang, W. Que, Metal Halide Perovskite Nanocrystals: Application in High-Performance Photodetectors, Materials Advances, Vol. 2, Iss. 3, 2021, pp. 856-879, https://doi.org/10.1039/D0MA00796J.
[15] H. Algadi, C. Mahata, B. Sahoo, M. Kim, W. G. Koh, T. Lee, Facile Method for the Preparation of High-Performance Photodetectors with A Gqds/Perovskite Bilayer Heterostructure, Organic Electronics, Vol. 76, pp. 105444, https://doi.org/10.1016/j.orgel.2019.105444.
[16] K. Shen, X. Li, H. Xu, M. Wang, X. Dai, J. Guo, T. Zhang, S. Li, G. Zou, K. L. Choy, I. P. Parkin, Z. Guo, H. Liu, J. Wu, Enhanced Performance of Zno Nanoparticle Decorated All-inorganic $Cspbbr_3$ Quantum Dot Photodetectors, Journal of Materials Chemistry A, Vol. 7, No. 11, 2019, pp. 6134-6142, https://doi.org/10.1039/C9TA00230H.
[17] W. Yang, J. Chen, Y. Zhang, Y. Zhang, J. He, X. Fang, Silicon-Compatible Photodetectors: Trends to Monolithically Integrate Photosensors with Chip Technology, Advanced Functional Materials, Vol. 29, Iss. 18, 2019, pp. 1808182, https://doi.org/10.1002/adfm.201808182.
[18] Y. Yang, F. Gao, Q. Liu, J. Dong, D. Li, X. Luo, J. Guo, J. Shi, Y. Lin, W. Song, X. Wang, S. Li, Long and Ultrastable All-Inorganic Single-Crystal $CsPbBr_3$ Microwires: One-Step Solution In-Plane Self-Assembly at Low Temperature and Application for High-Performance Photodetectors, Journal of Physical Chemistry Letters, Vol. 11, No. 17, 2020, pp. 7224-7231, https://doi.org/10.1021/acs.jpclett.0c01920.
[19] L. Zhou, K. Yu, F. Yang, H. Cong, N. Wang, J. Zheng, Y. Zuo, C. Li, B. Cheng, Q. Wang, Insight Into The Effect of Ligand-Exchange on Colloidal $CsPbBr_3$ Perovskite Quantum dot/Mesoporous-TiO_2 Composite-based Photodetectors: Much Faster Electron Injection, Journal of Materials Chemistry C, Vol. 5, No. 25, 2017, pp. 6224-6233, https://doi.org/10.1039/C7TC01611E.
[20] J. Miao, F. Zhang, Recent Progress on Highly Sensitive Perovskite Photodetectors, Journal of Materials Chemistry C, Vol. 7, Iss. 7, 2018, pp. 1741-1791, https://doi.org/10.1039/C8TC06089D.
[21] T. T. Duong, T. D. Tran, Q. T. Le, CNC Assisted Spray Deposition of Large Grain Size $CH_3NH_3PbI_3$ Film for Perovskite Solar Cells, Journal of Materials Science: Materials in Electronics, Vol. 30, No. 12, 2019, pp. 11027-11033, https://doi.org/10.1007/s10854-019-01444-4.
[22] C. Weerd, J. Lin, L. Gomez, Y. Fujiwara, K. Suenaga, T. Gregorkiewicz, Hybridization of Single Nanocrystals of Cs_4PbBr_6 and $CsPbBr_3$, Journal of Physical Chemistry C, Vol. 121, No. 35, 2017, pp. 19490-19496, 10.1021/acs.jpcc.7b05752.
[23] T. T. Duong, P. H. Hoang, L. T. Nhan, L. V. Duong, M. H. Nam, L. Q. Tuan, Multistep Spin–spray Deposition of Large-grain-size $CH_3NH_3PbI_3$ with Bilayer Structure for Conductive-carbon-based Perovskite Solar Cells, Current Applied Physics, Vol. 19, No. 11, 2019, pp. 1266-1270. 10.1016/j.cap.2019.08.014.
[24] P. N. Tran, B. D. Tran, D. C. Nguyen, T. L. Nguyen, V. D. Tran, T. T. Duong, A Facile Centrifuge Coating Method for High-performance $CsPbBr_3$ Compact and Crack-free Nanocrystal Thin Film Photodetector, Crystals, Vol. 12, No. 5, 2022, pp. 587, https://doi.org/10.3390/cryst12050587.